Locating Facial Landmarks Towards Plastic Surgery

Ricardo Teles Freitas, Kelson Rômulo Teixeira Aires
Departamento de Computação
Universidade Federal do Piauí
Teresina, Piauí, Brasil
ricard0tfreitas@gmail.com, kelson@ufpi.edu.br

Victor Eulálio Sousa Campelo
Clínica Otocenter
http://www.clinicaotocenter.com.br
dr.vcampelo@gmail.com

***Abstract*—The improvement of digital cameras and computers' processing capabilities have made applicable the solutions of a wide range of problems regarding image processing and computer vision. Among the most interesting tasks in this field of expertise, there are several face related problems. Many works have been proposed to solve problems such as face recognition, expression and age estimation, facial reconstruction, etc. Those works have a large potential to be explored in applications ranging from computer graphics to security and, even, medical software.**

This work proposes a method to automatic locate and identify a set of facial landmarks. The goal is to quickly provide precise and helpful information for plastic surgery procedures. The proposal, after implemented and tested on over 400 images, presented encouraging results for aesthetic analysis. Besides, it brings a novel methodology to locating specific landmarks needed for planning surgeries.

***Keywords*-Facial landmarks; Plastic surgery**

I. Introduction

The human face provides fairly information about a person, therefore, many computational solutions have been proposed to solve face related problems. In biometrics, for instance, it is possible to evaluate those features to perform several tasks related to face detection and recognition [1] [2] [3], facial expression [4], age estimation and, even, gender classification [5] [6]. The interest in this area has significantly grown over the past decades as pointed out by Jafri, Arabnia [7] and Yang et al. [8].

In fact, general facial features are crucial to solve biometric problems. In addition, facial landmarks also play an important role regarding those issues. In their work, Shi et al. introduce a concern about the increasing size of data-sets for face recognition [9]. Their work proposes a method based on landmarks and their geometry to reduce face search spaces. Besides, they suggest their method is efficient for direct face recognition. Senaratne and Halgamuge [10] proposed an optimization for their own method based on facial landmarks to solve the problem of face recognition. Their proposal was inspired by deformable methods such as Elastic Bunch Graph Matching and Active Shape Model.

Facial landmarks are also essential for another field of knowledge. In medicine, they hold fundamental information about a patient's face. Surgeons need to be aware of all the parameters and procedures required to fix or improve a patient's face. Therefore, they must be certain of all the needed landmarks and their spatial relations, among other important data.

Many works have proposed not only different sets of facial points to help planning surgeries, but also several metrics in order to evaluate and choose the best procedures. Prendergast [11] presents a variety of metrics based on soft tissue landmarks to evaluate the beauty of a human face. Zimbler and Ham [12] point out that facial analysis depend on both skeletal and soft tissue anatomic landmarks. The result of such analysis is fundamental for a successful surgical procedure planning.

The main motivation of this work is to quickly provide reliable data for planning surgeries. This work proposes an automatic method for locating and identifying facial landmarks, in order to make possible facial analysis that help planning surgical procedures.

A. Overview

The proposed method is based on local features of the profile image. These features can be distinguished by contour patterns that were identified and used to locate the facial landmarks needed for aesthetic analysis. The method was implemented and tested using 400 different profile images. The results were compared with a manual identification performed by two experts.

Considering related works, none of them shares more similarities with this one as Bottino and Cumani's work [13]. Their proposal is to determine facial landmarks in profile images. Their segmentation's uses histogram analysis to detect the face profile and the points based on information of local curvature from the profile contour.

The approach adopted in this work is similar to Bottino and Cumani's method once it is also based on analysis of the profile contour curvature. The definition of the facial landmarks, with a few exceptions, suggests that this is the course of action. However, the way the analysis is conducted is different from Bottino and Cumani's method from the profile's segmentation to the points' localization. In addition, this work introduces a novel method for locating important landmarks needed for planning surgeries.

This paper is divided into five sections, including this one. Following, Section II presents a description of the target points covered. Section III describes the methodology applied to locate the facial landmarks. In Section IV there is a discussion on the tests and results of the method's implementation.

Finally, Section V is a conclusion of this work, presenting the difficulties related and future works.

II. Facial Points

The first fundamental aspect of this work is to select the target points. Plastic surgeons may have, according to their own needs, a specific set of points to perform their pre-operative analysis. However, there are certain facial landmarks commonly used by surgeons. For this work, profile contour points, as defined by Prendergast [11], Zimbler and Ham [12], were chosen. Figure 1 shows the location of each point in the profile image. They are:

1) **Trichion** - anterior hairline in the midline;
2) **Glabella** - the most prominent part in the midline between the brows;
3) **Nasion** - the root of the nose in the midline;
4) **Rhinion** - soft-tissue correlate of the osseocartilaginous junction on the nasal dorsum;
5) **Tip** - the most anterior part of the nose;
6) **Columella** - connects the apex of the nose to the philtrum of the cutaneous upper lip;
7) **Subnasale** - the junction of the columella and upper cutaneous lip;
8) **Superior Labrum** - the junction of the red and cutaneous parts of the lip;
9) **Stomion** - the point where the lips meet in the midline;
10) **Inferior Labrum** - the point in the midline of the lower lip at the vermilion border;
11) **Supramentale** - midpoint of the labiomental crease between the lower lip and chin;
12) **Pogonion** - the most anterior point of the chin;
13) **Menton** - the most inferior point of the chin;
14) **Cervical** - the innermost point between the submental area and the neck.

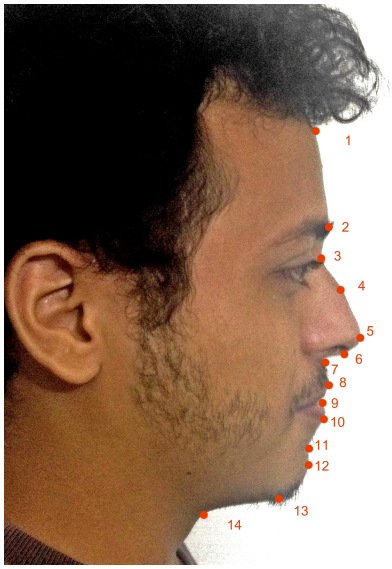

Fig. 1. Target points.

III. Methodology

The proposed method was developed to work on images under certain conditions that must be acquired in a controlled ambient:

- the image must contain only one face profile;
- the profile must be in the natural horizontal position;
- the background must be a contrasting and uniform color.

One could argue that those conditions are very limiting and are not often faced in the real world. There are algorithms that approach the problem of locating faces in the wild, such that one proposed by Zhu et al. [14], and they are, therefore, more appropriate for a real environment.

However, for the concerns of this work, a controlled ambient for image acquisition is more convenient. The better the image quality, the more accurate the algorithm will be. In Section IV there is a discussion about how accuracy is more relevant over other measures that enforces the need for a good image acquisition.

Figure 2 is an overview of the algorithm in all stages. The input image goes through several steps of processing until the points' localization.

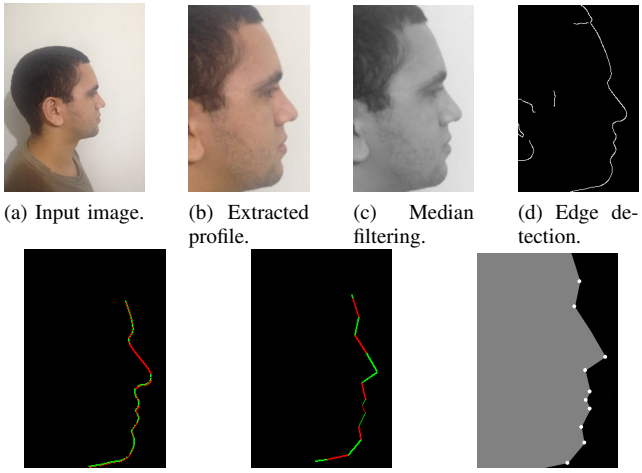

(a) Input image. (b) Extracted profile. (c) Median filtering. (d) Edge detection.

(e) Contour tracing. (f) Contour simplification. (g) Point localization.

Fig. 2. Method's stages.

A. Locating the Profile

An important aspect of this work is to detect and locate a face in the image. There are a great amount of techniques, described in the literature, to solve the problem of face detection and recognition in images [15] [16]. Some of them make use of key points to detect the face.

Binefa et al. [17] take into account both precision and time as requirements when they proposed an approach aimed to locate facial points in video images. Zhu et al. [14] presented a more complete work, that involves face detection, pose estimation and landmark localization.

The first step is detecting and locating the profile. Once located, the face profile is separated from the rest of the image. For such purpose, the method proposed by Zhu et al. [14]

was chosen. This approach uses pre-defined models of the human face to estimate pose in the image. It is capable to identify several poses in different angles. The algorithm was put easily available in MATLAB® code which contributed to its adoption.

The result of this method's application is a set of facial points. These points represent facial features of the located profile. They vary, horizontally, from the beginning of the mandible to the tip of the nose and vertically from the eyebrow to the chin.

Given that information, only the points lying on the edges of the face are extracted:

- (x_t, y_l) - Top left corner;
- (x_t, y_r) - Top right corner;
- (x_b, y_r) - Bottom right corner;
- (x_b, y_l) - Bottom left corner.

Figure 3 shows how the corner points are calculated from the extracted profile.

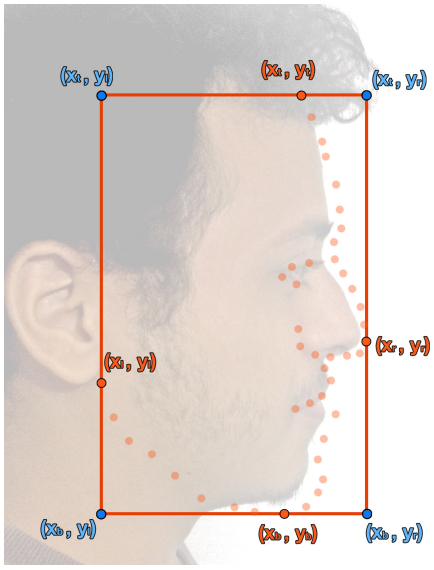

Fig. 3. Profile segmented.

Though the algorithm used to locate the profile presents good results, in some cases the profile border points retrieved are mislocated. That may exclude some important landmarks. To solve this issue, the profile borders were extended as follows:

$$y'_r = y_r + (y_r - y_l) \times 0.13 \quad (1)$$

$$y'_l = y_l \quad (2)$$

$$x'_t = x_t - (x_b - x_t) \times 0.6 \quad (3)$$

$$x'_b = x_b + (x_b - x'_t) \times 0.04 \quad (4)$$

Those values were chosen to define the new profile borders. The extension was large enough to make sure the actual profile would safely fit inside the new border. Those values were found after analyzing a set of 30 different profile images that were not used to evaluate this method, since they are part of this work's formulation. Figure 4(a) shows how inaccurate profile detections can be after the algorithm's application. In this case, the tip of the nose lies out of the detected profile region. Figure 4(b) presents of a new set of corners, calculated from the equations above, to define the profile border. This new profile segmentation contains all the target points.

(a) Wrong profile detection.

(b) Extended profile.

Fig. 4. Profile segmentation.

B. Processing the Profile Image

Since the method proposed is highly dependent on contour analysis, the segmented profile must be processed in order to extract the edges. The first stage of this process is the image smoothing. This process had to be performed to remove image's undesired artifacts, such as background objects that could be interpreted as edges.

In this work, because of it's low computational cost and satisfactory results, the median filter, with 3x3 kernel, was used to reduce image's noise. After filtering process, the image is converted to gray scale.

Finally, the edges must be extracted from the resulting gray scale image. There are several methods to perform this task, so, an experiment had to be conducted to choose the best approach. The experiment considered Sobel [18], Prewitt [19] and Canny [20] methods with a set of different parameters. The results were compared and Canny's approach presented the best results, regarding the needs of this work.

After this process, the resulting image I_{bin} (binary image) contains only the edges of the profile.

C. Simplifying the Profile Contour

This is the key point of the algorithm. Suppose there is a set S of pixels composed by the profile contour pixels. The landmarks, by definition, can be found on the profile contour, therefore, all of them belong to S. The challenge is to find a subset of S consisting only of the desired landmarks. The simplification process will reduce the initial set S to a much smaller one (i.e. find a subset of S). Thus, it will constrain the search field, leaving only the candidate landmarks.

Bottino and Cumani analyze the profile's points curvatures using the first and second order derivatives, evaluated by convolution with isotropic Gaussian derivative kernels [13]. This work approaches the problem in a different way. The

process of contour simplification will reduce the set of candidate landmarks at each iteration of the algorithm. This is done until only the most important points are found.

1) Determining the Contour: the first stage to simplify the contour is to extract it from the image I_{bin}. First of all, the image is divided vertically into three slices of same height $(x'_b - x'_t)/3$. The first point located is the nose tip, which is in the middle slice. This point will be the landmark that will guide the location of the profile contour.

Considering an image that meets the requirements pointed out in the beginning of the section, the tip of the nose (px, py) is the pixel far right or left, depending on which side the head is turned to, in the image. Since the algorithm of Zhu et al. [14] estimates head pose, it is possible to immediately locate this point.

Suppose that each pixel, with intensity greater than 0 in I_{bin}, represents a vertex of a graph G. The edges are the connections between two neighboring vertexes (i.e. two adjacent pixels with intensity greater than 0). Then, starting at the tip, a graph search is performed to find all the pixels of the contour. If the conditions described in the beginning of this Section are respected, each vertex of G will, likely, have only two edges. Some cases where the image acquisition is not ideal present some extra difficulties. Those are described in Section IV.

This search ends when there are no more vertexes to find. The process captures the contour and stores it in a list of ordered pairs $C_p = p_1, p_2, .., p_n$, where $p_i = (x, y)$ is the pixel location.

2) Transforming the Contour into Vectors: simplifying the contour consists in selecting the pixels that, together, represent the most important features of the profile. In this stage, some pixels are discarded and the remaining ones indicate the rough location of the target points.

To achieve this result, the strategy employed takes advantage of the analytical geometry's concept of vector addition. The idea is to turn the list of pixels C_p into a collection of points, where consecutive pixels represent, respectively, the initial and terminal points of the vector. The Algorithm 1 specifies this transformation.

Data: C_p
Result: L_v
foreach p_i *and* p_{i+1} *in* C_p **do**
  /* $\vec{v_i}$ starts at p_i and ends at p_{i+1} */
  $\vec{v_i} \leftarrow [p_i, p_{i+1}]$;
  Add v_i in L_v;
end
foreach $\vec{v_i}$ *and* $\vec{v_{i+1}}$ *in* L_v **do**
  if $\vec{v_i}$ *and* $\vec{v_{i+1}}$ *have the same direction* **then**
    $\vec{v_{i+1}} \leftarrow \vec{v_i} + \vec{v_{i+1}}$;
    Remove $\vec{v_i}$ from L_v;
  end
end

Algorithm 1: The contour C_p is converted to a list L_v of vectors. Consecutive vectors facing the same direction are added.

The procedure turns the profile into a list of vectors keeping all the features of the contour C_p. However, it is necessary to keep only the features that matter most, by disposing of some vectors from the list L_v.

3) Selecting Vectors: it's essential removing some points of the contour, in order to easily locate the local features. But selecting the right points turns out to be a problem, because, certain points play a very important role to define some features. If the wrong points are picked, the profile may lose it's most important features and that would compromise the method's accuracy.

This is the stage where the concept of vector addition becomes helpful. Choosing the points that will leave the contour C_p is done by sequentially adding vectors in the list L_v. When two vectors $\vec{A}$ and $\vec{B}$ are added, they are replaced by their sum in the list L_v. Consequently, the terminal pixel of vector $\vec{A}$ (or initial pixel of vector $\vec{B}$) is lost, making the contour C_p simpler. Of course there has to be a limit for the sequential additions, otherwise all the features will be lost.

That limit is controlled by a threshold that indicates if two vectors can be added. The threshold considers the information lost when two vectors are summed. This amount of information is measured in pixels. Figure 5(a) shows a subset of S with only 3 pixels (out of 8 initially), represented by black squares. After adding the vectors in Figure 5(a), whose magnitudes added equals 7, there is a resulting one of magnitude equals 5. The amount of information that is used, along with the threshold, to control the simplification process is the difference between those values. If that value exceeds the threshold, the vectors are preserved and the pixel remains in the subset. Otherwise, they are summed and the pixel leaves the subset. In Figure 5(b) the rightmost pixel is discarded.

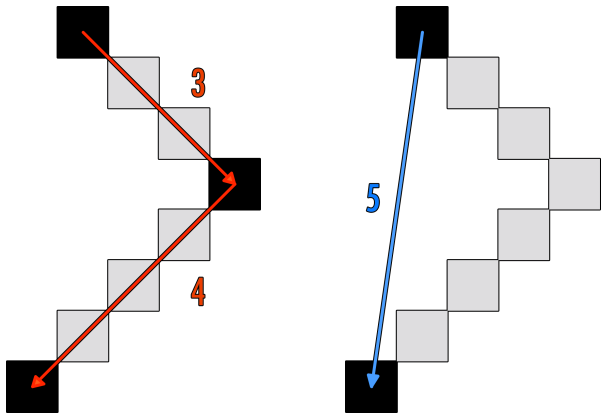

(a) Original vectors (b) Resulting vector

Fig. 5. Vector addition.

In addition, since this process is iterative, it's important to keep track about the information that sum of vectors took from the contour. Therefore, those values must be accumulated and used to control the process.

D. Locating the Points

By adjusting the threshold's value it's possible to reduce the contour C_p to a set of pixels very similar to the actual

desired profile landmarks. Several threshold values were tested to come up with a satisfactory answer for this issue. However, due to a large variety of profile contours, a static value for this parameter is not advised. To solve this issue properly, the threshold value is dynamic and changes according to the profile.

The threshold is initially set to a value small enough to keep C_p unchanged. As this value is insufficient to allow the landmarks location, it has to be increased. To control this value, the pixels in C_p must be grouped according to their corresponding vectors in L_v. They are grouped based on the angles A_i (where i means an index in list L_v) formed by two consecutive vectors in L_v. Subsequent pixels whose angle A_i is acute belong to the same group. If the angles are obtuse, they belong to another group.

This method divides C_p into several groups, since those angles alternate between acute and obtuse along the profile contour. That information is responsible for changing the threshold value, that must be reset until the amount of groups meets the number of local extrema of a regular human profile.

Given this threshold, each remaining group of pixels in C_p holds exactly one candidate landmark (except for Menton and Pogonion, that belong to the same group). Then, to identify the target points it's just necessary to perform a simple analysis within those groups.

Figure 6 shows the location of the points on the resulting contour. The features of each point match with the pixels in C_p.

Fig. 6. Processed profile contour.

IV. Results and Discussion

The method was implemented in Objective-C to evaluate it's accuracy. To design the algorithm, 30 different images were used. The tests were made in 400 different image profiles, all of them under the conditions presented in section III. The results were compared to ground truth markings performed by two experts.

A. Measurements

The Euclidean geometry was chosen to measure the distance (error) between manually and automatically located landmarks. Before compiling the results, the distances raw information must be put in perspective. The actual distance between the markings may deceive because the images are not the same size. This means those absolute differences may be more or less significant, that will depend on the image's size.

The approach adopted in this work to evaluate test results takes into account not only the absolute differences between markings, but, also, their relation with the image's size. Table 1 shows the absolute average distance, the standard deviation and one relation considering the image's size.

TABLE I
Measurements in test images of 2536 x 3456 resolution.

Point	**Avg Error (px)**	**Standard Deviation**	**Avg / Image Size (10^{-6} %)**
Trichion	216.71	9.48	27.57
Glabella	66.26	7.93	8.81
Nasion	67.12	2.29	9.32
Rhinion	81.40	6.98	11.23
Tip	8.93	0.75	1.19
Collumela	45.57	5.77	6.16
Subnasale	23.14	0.98	3.13
Superior Labrum	36.97	2.12	4.89
Stomion	22.60	1.11	3.05
Inferior Labrum	29.80	1.24	4.09
Supramentale	30.30	1.87	4.13
Pogonion	38.90	3.97	5.20
Menton	80.06	5.31	10.91
Cervical	206.70	9.20	27.75

B. Measurements Discussion

The best results match the points where the local curvature is more obvious. Tip, subnasale and stomion are, in most cases, very apparent local extremes on the contour, thus, their automatic location present the best results. Superior and inferior labrum, supramentale and even nasion were reasonably well identified.

Trichion and cervical are the most challenging landmarks. Their automatic location presented inconsistent results that could hardly be used in a real profile analysis. However, the testing images presented some extra challenges that made those landmarks' location harder, even for the experts.

According to the definition presented in Section II, the trichion lies on the hairline. In some images, this point is hidden by the individual's hair or, even worse, there is no hairline apparent (occasionally caused by baldness). In those cases, this landmark's location is very difficult.

Cervical location also has an obstacle. This point can easily be located in younger people. However, the elderly are more likely to present a double chin, which hides the cervical. In

those cases, even the experts disagreed when locating this landmark.

Figure 7 gives a good idea of the method's average accuracy. It shows one test case with points manually marked. The radius of each point represents it's average error, therefore, smaller circles indicates more accurate markings.

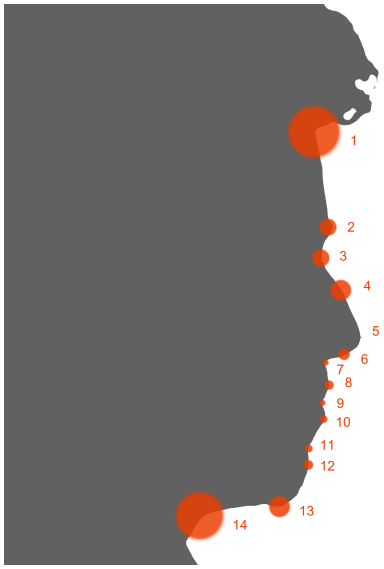

Fig. 7. Average error graphically.

Related works, such as Bottino and Cumani's [13], usually measure the error using an absolute value of pixels. This approach was also adopted in this work to give a rough notion on the average error. However, the comparison of the two works, regarding this approach, becomes unfair as the set of images are different. Bottino and Cumani's work used a set of small images (480 x 640 pixels), whereas this work used, mostly, very large images (2536 x 3456 pixels).

C. Threshold Discussion

The threshold, presented in Section III, is a direct responsible over the amount of lost features. The higher it's value the more features are lost and simpler the contour becomes. This process preserves consecutive vectors whose direction's difference is greater. So, the threshold value must be carefully set in order to reduce the contour C_p only to it's most important pixels.

Figure 8 shows different threshold values being applied to the same contour. In Figure 8(b), the threshold is zero, no feature is lost. In Figure 8(c), the threshold helps keeping the most important features for this work's purpose, thus, it is considered a good value. In Figure 8(d) the threshold is very high, resulting in a much simpler contour.

D. Accuracy Relevancy

It appears trivial to presume that accuracy is important for any work regarding landmark location. There is no doubt it is an important measure. But for this work's motivation it means more than a way to compare related works and to evaluate

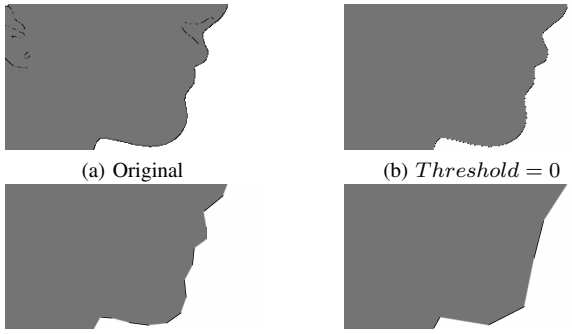

(a) Original (b) $Threshold = 0$

(c) $Threshold > 0$ (d) $Threshold >> 0$

Fig. 8. Region under the nose.

a methodology. To understand why accuracy is so relevant over other measures, in this context, let's analyze one of the most important aspects of rhino-plastic surgery, as stated by Crumley and Lanser [21], which is the surgical alteration of nasal tip projection.

One of the most cited metrics to evaluate nasal tip projection is called the Baum ratio. It is calculated by dividing the length of a line A from the nasion to the subnasale by the length of a perpendicular line B from the nasal tip to a vertical line from the subnasale [11]. Powell and Humphreys [22] say the ideal Baum ratio is 2.8 and a discrepancy of -5% on this value means the nasal tip is over projected.

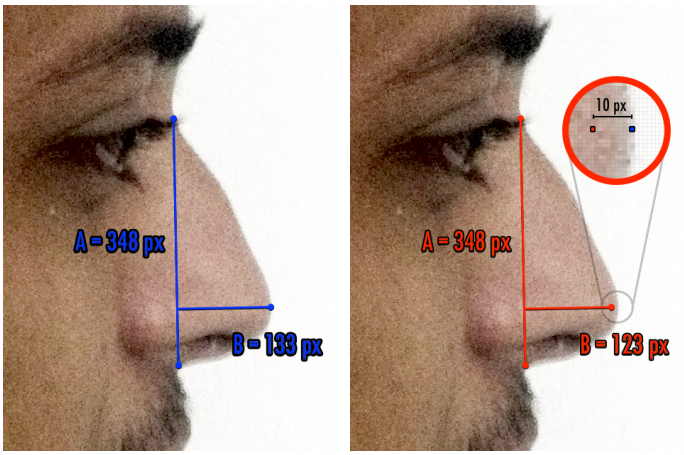

(a) Correct location. (b) Wrong location.

Fig. 9. A misplacement of only 10 pixels left of the correct tip location causes the Baum ratio to increase from 2.6 to 2.8. That would mean this nose's tip is ideal, which is not correct.

Figure 9 shows two different nose tip locations. In Figure 9(a), the tip is considered over projected since it's Baum ratio equals 2.61. But in Figure 9(b), where the landmark was wrongly located 10 pixels left of it's correct spot, the Baum's ratio increases up to 2.82. Considering the size of this image, this misplacement is visually hard to notice. However, it is large enough to make a wrong evaluation of the patient's nose. In other situations, such mistake could end, in the worst cases, in an unnecessary surgery with really undesired results.

Considering this work's motivation, accuracy is more rele-

vant than computational cost, execution time and robustness. That is why a good image acquisition performed in a controlled ambient is so important. In fact, for this work's purpose, such an ambient is exactly the expected place this method should work, since it will be used in a doctor's office or in a hospital.

E. Contour Issues

This work proposes a method highly dependent on edge detection. Therefore, any problem related to contour extraction has a great influence on the results. A dark background, for instance, can easily blend with the individual's eyebrow or hair making very hard the task of locating the nasion or the trichion. The graph search approach adopted to extract the profile demands a flawless contour, which leaves a great possibility for failure and bad results.

Some other works can be used to solve the problem of contour extraction. Active Contour Models [23] is an example of technique that can be explored in future works to make this algorithm more robust and less dependent on a perfect edge detection. It uses an energy-minimizing spline to find some features such as lines and edges.

V. Conclusion

The proposed method is a simple and effective alternative to locate facial landmarks on the profile's contour. It introduced a novel method to locate landmarks such as the rhinion and the columella. Test results indicate the method can be compared to ground truth location for some landmarks such as the nose tip, stomion and subnasale. On the other hand, trichion and cervical location is very hard and presented bad results.

In order to perform a complete facial aesthetic analysis, it's necessary to locate a wider set of facial landmarks. Future works must not only consider perfecting the current method but, above it all, they must focus their efforts in locating landmarks in frontal images since this work only regards the profile contour.

One of the most remarkable difficulties was to deal with the diversity of analyzed faces. The face landmarks' definitions found in the literature work as a guide to plastic surgeons. However, given the differences between human faces, those definitions are not always applicable. In some cases the features were presented very obvious, but in others they were extremely subtle. To overcome this obstacle was one of the greatest challenges of this work.

Another problem regards the contour extraction. Since this method is based on edge detection, there may be some issues with the image background. Depending where the image was acquired, the background can blend with the profile, causing some terrible effects over the results. Future works should make the contour extraction more robust to those variations. Some works, such as Active Contour Models, can be used to solve similar issues.

References

[1] R.-L. Hsu, M. Abdel-Mottaleb, and A. K. Jain, "Face detection in color images," *IEEE Transactions on Pattern Analysis and Machine Intelligence*, vol. 24, no. 5, pp. 696–706, May 2002.

[2] P. Belhumeur, J. Hespanha, and D. Kriegman, "Eigenfaces vs. fisherfaces: Recognition using class specific linear projection," *IEEE Transactions on Pattern Analysis and Machine Intelligence*, vol. 19, no. 7, pp. 711–720, July 1997.

[3] M. Turk and A. Pentland, "Face recognition using eigenfaces," in *IEEE Conference on Computer Vision and Pattern Recognition*. IEEE, 1991, pp. 586–591.

[4] M. Pantic and L. Rothkrantz, "Automatic analysis of facial expressions: the state of the art," *IEEE Transactions on Pattern Analysis and Machine Intelligence*, vol. 22, no. 12, pp. 1424 – 1445, December 2000.

[5] D. Cao, C. Chen, M. Piccirilli, D. Adjeroh, T. Bourlai, and A. Ross, "Can facial metrology predict gender?" in *Proceedings of International Joint Conference on Biometrics*, 2011.

[6] B. Moghaddam and M.-H. Yang, "Gender classification with support vector machines," in *Proceedings of the 4th IEEE International Conference on Face and Gesture Recognition*, March 2000.

[7] R. Jafri and H. R. Arabnia, "A survey of face recognition techniques," *ournal of Information Processing Systems*, vol. 5, no. 2, pp. 41–68, June 2009.

[8] M.-H. Yang, D. J. Kriegman, and N. Ahuja, "Detecting faces in images: A survey," *IEEE Transactions on Pattern Analysis and Machine Intelligence*, vol. 24, no. 1, pp. 34–58, January 2002.

[9] J. Shi, A. Samal, and D. Marx, "How effective are landmarks and their geometry for face recognition?" *Computer Vision and Image Understanding*, vol. 102, no. 2, pp. 117–133, May 2006.

[10] R. S. Senaratne and S. K. Halgamuge, "Optimal weighting of landmarks for face recognition," *Journal of Multimedia*, vol. 1, no. 3, pp. 31–41, June 2006.

[11] P. M. Prendergast, *Advanced Surgical Facial Rejuvenation*, 1st ed. Springer-Verlag Berlin Heidelberg, 2012, ch. Facial Proportions, pp. 15–22.

[12] M. S. Zimbler and J. Ham, *Cummings Otolaryngology - Head and Neck Surgery*, 5th ed. Elsevier Health Sciences, 2010, ch. Aesthetic Facial Analisys.

[13] A. Bottino and S. Cumani, "Robust identification of face landmarks in profile images," in *Proceedings of the 12th WSEAS international conference on Computers*, 2008, pp. 107–114.

[14] X. Zhu and D. Ramanan, "Face detection, pose estimation, and landmark localization in the wild," in *IEEE Conference on Computer Vision and Pattern Recognition*. IEEE, 2012, pp. 2879 – 2886.

[15] C. Fernandez and M. A. Vicente, "Face recognition using multiple interest point detectors and sift descriptors," in *8th IEEE International Conference on Automatic Face and Gesture Recognition*, 2008, pp. 1–7.

[16] H. Changbo, J. Harguess, and J. Aggarwal, "Patch-based face recognition from video," in *IEEE International Conference on Image Processing*, 2009.

[17] M. F. Valstar, B. Martinez, X. Binefa, and M. Pantic, "Facial point detection using boosted regression and graph models," in *Conf. on Computer Vision and Pattern Recognition*, 2010, pp. 2729–2736.

[18] I. Sobel, "An isotropic 3x3 image gradient operator," in *Machine Vision for Three-dimensional Scenes*. Academic Press, 1990.

[19] J. M. S. Prewitt, "Object enhancement and extraction," in *Picture Processing and Psychopictorics*. Academic Press, 1970.

[20] J. Canny, "A computational approach to edge detection," in *IEEE Transactions on Pattern Analysis and Machine Intelligence*, 1986, pp. 679–698.

[21] R. L. Crumley and M. Lanser, "Quantitative analysis of nasal tip projection," *The Laryngoscope*, vol. 98, no. 2, pp. 202–208, 1988.

[22] N. Powell and B. Humphreys, *Proportions of the Aesthetic Face*, ser. The American Academy of Facial Plastic and Reconstructive Surgery. Thieme Medical Pub, 1984.

[23] M. Kass, A. Witkin, and D. Terzopoulos, "Snakes: Active contour models," *International journal of computer vision*, vol. 1, no. 4, pp. 321–331, 1988.